

The Tectonic Evolution of the Scotia Sea Region from the Cretaceous until today 1

Anouk Beniest¹, J H Oldenhage^{2,3}, W P Schellart², and A Beniest^{2,3}

¹Affiliation not available

²Faculty of Science, Department of Earth Sciences, Vrije Universiteit Amsterdam

³Department of Earth and Environmental Sciences

November 8, 2023

14 Abstract

15 The interplay between regional tectonics and the development of a major ocean gateway between the Pacific
16 and the Atlantic Ocean has resulted in numerous paleogeographic reconstruction studies that describe the
17 Cenozoic tectonic history of the Scotia Sea region. Despite the multitude of published tectonic
18 reconstructions and the variety of geological and geophysical data available from the Scotia Sea, the
19 geological history remains ambiguous. We present a comparative paleogeographic analysis of previously
20 published tectonic reconstructions to identify agreements and conflicts between these reconstructions and
21 we propose an alternative model to explain the Cenozoic evolution of the Scotia Sea region. The
22 paleogeographic comparison shows that most reconstructions agree on the tectonic evolution of the South
23 Scotia Ridge and the East Scotia Ridge. Major differences between the reconstructions are the role of the
24 westward subducting plate below the South American Plate, and the age and origin of the Central Scotia
25 Sea (CSS). Tectonic reconstructions assume that the CSS is either a part of a Cenozoic back-arc basin, or a
26 captured piece of Cretaceous oceanic crust. We propose a new alternative tectonic reconstruction that brings
27 these two prevailing hypotheses elegantly together. In our model, we identified new geographical units
28 consisting of thinned continental or Cretaceous oceanic fragments that originate from the Paleo Pacific –
29 Weddell Sea gateway from high-resolution bathymetry. These fragments are now part of the CSS and have
30 been affected by early back-arc tectonic activity of the South Sandwich subduction zone, leading locally to
31 the formation of Cenozoic-aged crust in the CSS.

32

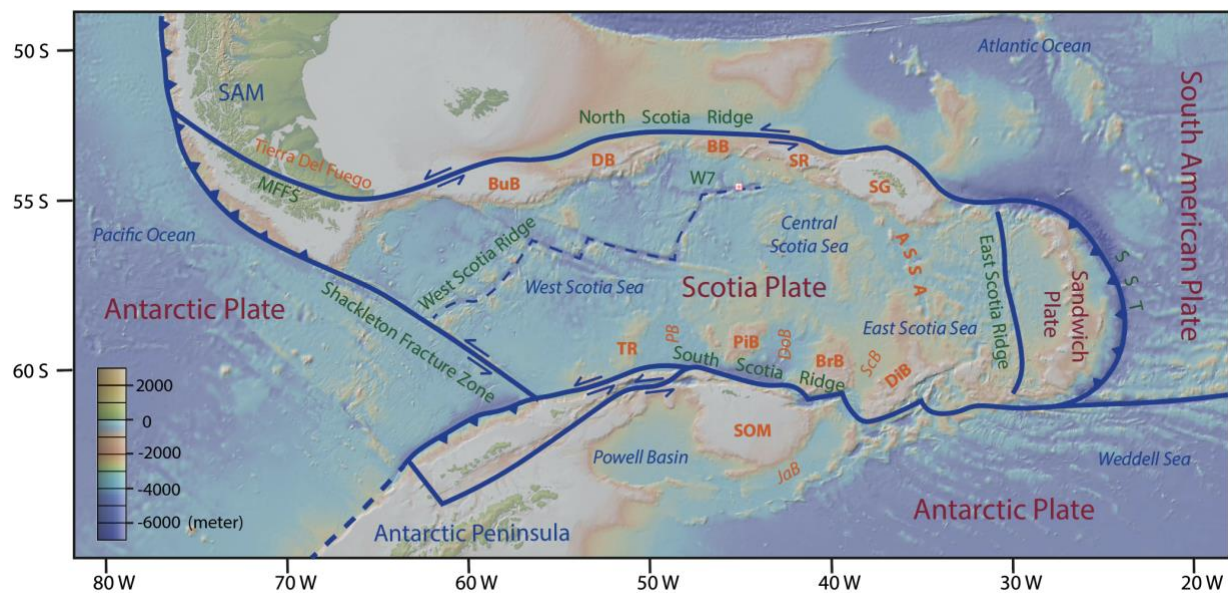
33 1. Introduction

34 The Eocene-Oligocene global cooling event occurred as a response to a decrease in atmospheric carbon
35 dioxide (CO₂) levels (Anagnostou et al., 2016; Pearson et al., 2009) and the onset of the Antarctic
36 Circumpolar Current (ACC, Sauermilch et al., 2021). The effect of both mechanisms on the Eocene-
37 Oligocene cooling event have been investigated thoroughly, with a dramatic cooling of the surface waters
38 recorded once the AAC formed deep-water currents (>300 m), demonstrating that tectonic changes, which

39 allowed the ACC to form, are of major importance for the Eocene-Oligocene cooling event (Sauermilch et
40 al., 2021). These tectonic changes involved the complex continental break-up of Southern Gondwanaland
41 during the Cenozoic, which led to the complete separation of the Antarctic continent and marked the onset
42 of the oceanic water current encircling Antarctica (ACC, Barker et al., 2007; Eagles et al., 2006; Eagles
43 and Jokat, 2014; Scher et al., 2015). The tectonic opening of both the Tasman Seaway, between the South
44 Tasman Rise south of Tasmania and Antarctica, and Drake Passage (Fig. 1), between South America (SAM)
45 and Antarctica (ANT), allowed the ACC to develop. The timing of the opening of the Tasman Seaway is
46 quite well constrained at around 32 Ma (Lawver & Gahagan, 2003), based on seafloor magnetic anomalies
47 and foraminifera in IODP drill cores (Bijl et al., 2013). This is unlike the opening of Drake Passage and the
48 formation of the Scotia Sea, for which the exact timing remains hotly debated, mostly because of the
49 region's complex tectonic evolution (Barker, 2001; Lawver & Gahagan, 2003; Livermore et al., 2007) and
50 its remote location, which resulted in scattered and incomplete datasets. Nevertheless, various authors have
51 suggested that the opening of Drake Passage played a key-role in the onset of the ACC (Dalziel et al.,
52 2013b; Kennett et al., 1977; Livermore et al., 2007; Whitworth, 1983).

53 The tectonic evolution of the Scotia region has been investigated in various studies over the past decades
54 (Barker, 1972; Barker, 2001; Dalziel, 1983; Dalziel et al., 2013, 2021; Eagles, 2000; Eagles et al., 2006;
55 Eagles & Jokat, 2014; Lagemaat et al., 2021; Livermore et al., 2007; Maldonado et al., 2014; Nerlich et al.,
56 2013; Pérez et al., 2016; Pérez et al., 2017; Pérez et al., 2019; Schellart et al., 2023; Vérard et al., 2012; De
57 Wit, 1977). These studies do not provide a unanimous view on the tectonic evolution of the Scotia region,
58 and consequently, they dedicate a different origin and evolution to the major structures in this area, i.e. the
59 South Sandwich subduction zone, the adjacent crustal fragments, Drake Passage and the Central Scotia Sea
60 (CSS, Fig. 1). The most striking differences between publications are the age and origin of the CSS. At first
61 the CSS was thought to be a back-arc basin that opened during the Cenozoic (Barker, 1970). Several years
62 later, De Wit (1977) proposed that the CSS originated from a Cretaceous back-arc basin. Later still,
63 Livermore et al. (1994) suggested that the CSS could have been the oldest piece of crust found in the Scotia
64 arc, that might pre-date the opening of Drake Passage. This idea (Livermore et al., 1994) was adopted by

65 (Eagles, 2010b) and reworked into a plate tectonic reconstruction (Eagles & Jokat, 2014). Both end-
 66 members, the Cenozoic back-arc basin and the captured piece of Cretaceous crust, are still being used in
 67 plate-tectonic reconstructions of the Scotia Sea (Dalziel et al., 2013a; Eagles, 2016; van de Lagemaat et al.,
 68 2021) but no scientific consensus has yet been reached about the age and origin of the CSS.
 69 The aim of this study is to test a more inclusive hypothesis about the age, origin and extent of the CSS,
 70 using observational constraints and published reconstructions. We evaluate the question whether the CSS
 71 region can consist of remnant pieces of Cretaceous oceanic crust that have experienced back-arc extension
 72 during the Cenozoic. We hypothesize that these crustal remnants originate from a gateway that once
 73 connected the Paleo Pacific Ocean and the Weddell Sea, the so- called Paleo Pacific-Weddell Sea (PPWS)
 74 gateway.



75
 76 **Figure 1:** Bathymetric map of the Scotia Sea region (bathymetry obtained from GeoMapApp (Ryan et al.,
 77 2009)) and present-day tectonics (adapted from Riley et al., 2019). *Abbreviations of the bathymetric high*
 78 *and lows are given in orange. North Scotia Ridge (NSR): BuB-Burdwood Bank; DB-Davis Bank; BB-Bruce*
 79 *Bank; SR-Shag Rocks, SG-South Georgia. South Scotia Ridge (SSR): TR-Terror Rise; PB- Protector Basin;*
 80 *PiB-Pirie Bank; DoB-Dove Basin; BrB-Bruce Bank; ScB-Scan Basin; DIB-Discovery Bank; SOM-South*
 81 *Orkney Microcontinent; JaB-Jane Basin.*

82 **2. Geological outline**

83 The Scotia region consists of five plates (Fig. 1): the South American plate (SAM), the Antarctic plate
84 (ANT), the Scotia plate (SCO), the South Shetland plate (SSh) and the Sandwich plate (Sa). The northern
85 boundary of the Scotia plate (SCO-SAM), the North Scotia Ridge (NSR), is a left-lateral strike-slip fault
86 (Smalley et al., 2007). The eastern boundary (SCO-SSa), the East Scotia Ridge (ESR) is an active spreading
87 centre (Barker, 1972), whereas the southern to south-western boundary (SCO-ANT), consisting of the
88 South Scotia Ridge (SSR) and the Shackleton Fracture zone (SFZ) classifies as a left-lateral strike-slip
89 system (Fig. 1). The SSa, east of the SCO, is confined in the north and east (SSa-SAM) by the South
90 Sandwich Trench (SST). Here, the South American plate subducts below the SSa. The southern plate
91 boundary of the SSA (SSa-ANT) is a right-lateral strike-slip fault.

92 The Scotia plate formed throughout the Cenozoic and consists of a multitude of basins and elevated crustal
93 fragments that define the present-day bathymetry. The largest basin, the West Scotia Sea in the west of the
94 Scotia Plate, formed along the extinct spreading centre of the West Scotia Ridge (WSR, Fig. 1, Barker and
95 Burrell, 1977). Several smaller basins and rises are located along the SSR. From west to east these are
96 Protector Basin, Terror Rise, Dove Basin, Pirie Bank, Scan Basin, Discovery Bank and Jane Basin. The
97 NSR is dominated by elongated East-West oriented banks and rises, including Burdwood Bank, Davis
98 Bank, Barker Bank (previously referred to as 'Aurora Bank'), Shag Rocks and South Georgia. Numerous
99 smaller faults (Cunningham et al., 1998) that accommodate the strike-slip movements along the ridge are
100 present in and around the elevated banks. These banks are of Cretaceous age (Riley et al., 2019) or older
101 (Tanner, 1982). Riley et al. (2019) also suggested Cretaceous ages for the adjacent seafloor, which is
102 referred to as the W7 segment (Fig. 1). This is in contrast with the previous hypothesis that the W7 segment
103 formed as a result of Cenozoic seafloor spreading along the WSR (Eagles et al., 2005).

104 Westward subduction of the South American plate below the Sandwich plate has resulted in the opening of
105 the second largest basin of the Scotia plate, the East Scotia Sea, which initiated at least 15 Ma to 17 Ma
106 along the ESR and continues spreading today (Eagles & Jokat, 2014; Larter et al., 2003). The South

107 Sandwich volcanic arc (Heezen & Johnson, 1965; Pearce et al., 2014) formed on the Sandwich plate in
108 response to the subducting South American plate.

109 The central part of the Scotia plate is referred to as the Central Scotia Sea (CSS). Magnetic anomalies have
110 been identified in the CSS (Barker, 1970), which suggests the presence of oceanic crust and former seafloor
111 spreading. For the CSS the anomalies have proven difficult to interpret (Barker, 2001; Eagles, 2010b;
112 Eagles & Jokat, 2014; Hill & Barker, 1980). There are two different schools of thoughts for the origin of
113 this part of the Scotia plate, one assuming a Cretaceous age of the crust, the other assuming a Cenozoic age.
114 The Cretaceous model assumes that the CSS is a captured piece of Cretaceous oceanic crust that could be
115 a conjugate of the Weddell Sea (Dalziel et al., 2013; Eagles, 2010a, 2000; Eagles and Jokat, 2014).
116 According to this model, no inactive spreading ridge, nor median valley is expected on this piece of oceanic
117 crust. The Cenozoic model assumes that the CSS formed during the Cenozoic as a result of back-arc
118 spreading due to westward subduction of the South American Plate beneath the Scotia plate (e.g. Barker,
119 2001; Hill and Barker, 1980; Livermore et al., 2007; van de Lagemaat et al., 2021; Nerlich et al., 2013;
120 V  rard et al., 2012) According to this model, the age of the seafloor is relatively young, and an extinct
121 spreading ridge is to be expected.

122 Remnants of a volcanic arc, named the Ancestral South Sandwich Arc (ASSA, Fig.1) are found on the
123 eastern part of the CSS. This arc formed in response to the subduction of the South American plate during
124 the early Oligocene - late Miocene (Pearce et al., 2014). The associated subduction zone extended from
125 South Georgia towards the southernmost extent of Jane Bank (Pearce et al., 2014). The same subduction
126 zone is suggested as driving force for back-arc spreading in the CSS in the young Cenozoic model (Barker,
127 2001; Hill & Barker, 1980; Livermore et al., 2007; Pearce et al., 2014; P  rez et al., 2014).

128

129 **3. Methods**

130 In this study, existing paleogeographic reconstructions have been compared using the open-source
131 reconstruction software GPlates (Boyden et al., 2011). The reconstructions were remodelled in GPlates

132 after georeferencing the published images and importing them in GPlates. We chose the reconstructions of
133 Eagles and Jokat (2014) and Livermore et al. (2007) for the re-modelling and comparison (Fig. 2 and 3),
134 because 1) they present two contrasting scenarios for the tectonic evolution of the CSS and 2) they were
135 presented in such a way that allowed a quantitative comparison. Eagles and Jokat (2014) favour a
136 Cretaceous CSS, while Livermore et al., (2007) present a Cenozoic age and origin of the CSS. The latter
137 group of authors build further on reconstructions from older studies (Barker, 2001; Livermore et al., 2005).
138 The published images of the two reconstructions were digitized with the thin-spline method of the open-
139 source geographical information software QGIS (version 3.4, 2018), prior to loading into GPlates. The
140 advantage of the GPlates software is that it allows the computation of the rotation poles of a set of pre-
141 defined geological units according to geo-referenced figures of the existing studies. This makes it possible
142 to quantitatively compare different tectonic reconstructions. In GPlates, rotations of so-called polygons are
143 described in a rotation file. The polygons in this study are referred to as geological units (GUs). A GU
144 represents a static crustal fragment. There are no general rules for defining these GUs, resulting in a variety
145 of shapes of the same area in different reconstructions. For most GUs the difference in size between the
146 different reconstructions is in the order of tens of kilometres. In some cases, however, the shapes vary
147 greatly, for example the length of the GU representing Davis Bank defined by Lagemaat et al. (2021) at 10
148 Ma is almost half the size (200 km) of the same GU defined by (Barker, 2001) (380 km) at 10 Ma.
149 This study works with an independent set of GUs, to allow comparison between the different
150 reconstructions (Fig. 4, red GUs). The shapes of these GUs were defined based on the bathymetry (DBM-
151 BATDRAKE, Bohoyo et al., (2019), GEBCO 2014, Weatherall et al., (2015), South Sandwich Ridge, Leat
152 et al., (2016), South Georgia, Hogg et al., (2016)), magnetic anomalies (Eagles et al., 2005), seismic profiles
153 (Maldonado et al., 2006) and gravity anomalies (Sandwell et al., 2014.). After definition, the GUs were
154 rotated according to the georeferenced images. This resulted in two different rotation files that mimic the
155 rotations applied in Livermore et al. (2007) and Eagles and Jokat (2014). Rotations are relative to a fixed
156 Antarctic Peninsula to be consistent with the reconstructions of Eagles and Jokat (2014) and Livermore et
157 al. (2007).

158 The results of the comparison between these two distinct tectonic reconstructions highlight a significant
159 number of uncertainties and disagreements in the evolution of the Scotia Sea region. The uncertainties,
160 agreements and disagreements between the compared reconstructions (Eagles & Jokat, 2014; Livermore et
161 al., 2007) and other existing reconstructions (e.g. Dalziel et al., 2013a; Pearce et al., 2014; V  rard et al.,
162 2012) have been reinterpreted and visualized in a new tectonic reconstruction. Additional GUs were added
163 to the new reconstruction to explain gaps between the existing reconstructions, and we discuss the potential
164 origin of these additional GUs (Fig. 4, light grey GUs). The geometry of the GUs is defined following
165 bathymetric features such as bathymetric highs and lineations. Shapes were adjusted to avoid under- and
166 overlap of the GUs. The geometries of these GUs are not absolute. For the shapefile and the rotation file of
167 the new reconstruction, see supplementary data.

168

169 **4. Results**

170 The results of the comparison of the paleogeographic reconstructions (Fig. 2 and 3) yield the major
171 differences and similarities between the two end-member tectonic reconstructions for the Scotia Sea region.
172 The most striking difference between the reconstructions is the assumption for the age and origin of the
173 CSS. Eagles and Jokat (2014) present this part as a captured piece of oceanic crust that formed in the
174 Cretaceous, which would later become the CSS, whereas Livermore et al. (2007) explain this part as the
175 result of an east-west oriented spreading centre that existed during the Paleogene, which resulted in the
176 formation of the CSS. All reconstructions (Fig. 2 and 3), including the ones not used for the GPlates
177 comparison, agree on the general evolution of the SSR and the ESR although small differences exist. We
178 will highlight the most striking similarities and differences between the reconstructions of Livermore et al.
179 (2007) and Eagles and Jokat (2014) at different time steps (Fig. 2 and 3). Where possible, comparisons are
180 made with the other studies that are not included in our GPlates reconstructions.

181

182

183 **4.1 50 Ma- Configuration of the land bridge between South America and Antarctica**

184 During the Early Eocene (Fig. 2a and 2b), the South American continent and Antarctica were connected.
185 This connection can be described as a land bridge, that later broke apart in multiple pieces that can be found
186 on today's ocean floor of the Scotia Sea. During Early Eocene times this land bridge was confined by two
187 subduction zones, one on the eastern side and one on its western side. Both Livermore et al. (2007) (Fig.
188 2a) and Eagles and Jokat (2014) (Fig. 2b) agree on this. The subduction zone on the eastern side of the land
189 bridge has been interpreted by Eagles and Jokat (2014) to result from ongoing shortening along the
190 Endurance Collision Zone (ECZ).

191 The most apparent difference between the reconstructions is the age and origin of the CSS. Eagles and Jokat
192 (2014) argue that the CSS is of Cretaceous origin, thus their reconstruction includes a GU that represents
193 this CSS. South Georgia, which they connect to the CSS, is not included in the land bridge in their
194 reconstruction (Fig. 2b). The area in between the GUs of the land bridge, is referred to as Omond Land by
195 Eagles and Jokat (2014). While Eagles and Jokat (2014) have space between the geological units that were
196 part of the land bridge, the reconstruction of Livermore et al. (2007) could not be reproduced without
197 overlap of the GUs that are part of the land bridge (Fig. 4b). This is not apparent in the reconstruction of
198 Livermore et al. (2007) because their GUs are smaller than the GUs used for this study. The GUs could
199 have been smaller in the geological past due to later stretching. Dalziel et al. (2013a, 2021) advocate that
200 South Georgia was positioned close to the Southern Andes, in contrast with Livermore et al. (2007) and
201 even more so with Eagles and Jokat (2014) while the origin of the CSS is proposed by Dalziel et al. (2013a)
202 to be a Cretaceous conjugate of the Weddell Sea.

203 A last major difference at this time step is that the eastern margin of Tierra del Fuego is located ~150 km
204 more towards the east in the reconstruction of Eagles and Jokat (2014) (Fig. 2b) compared to the
205 reconstruction of Livermore et al. (2007) (Fig. 2a). The position of the GU of the South American plate in
206 the reconstruction of Livermore et al. (2007) in our comparison cannot be compared to the reconstruction
207 of Eagles and Jokat (2014) because the size of the South American plate is much smaller (app. 300km in
208 length, measured from east to west) than the size of the GU that is being used by Eagles and Jokat (2014).

209 In our comparison we therefore only use parts of the continental margins of Tierra del Fuego and the South
210 American plate that remain unchanged through time.

211

212 **4.2 40 Ma- First signs of extension in the future Scotia Sea**

213 Ongoing eastward retreat of the eastern subduction zone caused back-arc extension in the land bridge. Both
214 Eagles and Jokat (2014) and Livermore et al. (2007) reconstruct an east-west oriented opening of Dove
215 Basin, between Pirie Bank and Bruce Bank (Fig. 2c and 2d).

216 The location of the eastern margin of Tierra del Fuego is still 120 km apart between the different
217 reconstructions, and thus Dove Basin is located at different latitudes and longitudes in both reconstructions.

218 The extension in Dove Basin results in multiple sinistral strike-slip movements between the GUs.
219 Livermore et al. (2007) do not report these faults (Fig. 2c). The Burdwood transform fault accommodates
220 these strike-slip movements in the reconstruction by Eagles and Jokat (2014) (Fig. 2d).

221 In other reconstructions, the Scotia plate and the ASSA have already formed at this stage (Dalziel et al.
222 2013a, 2013b). In this case, the plate extends from 57W to 37W and is smaller than it is nowadays, because
223 the WSR did not form yet (Dalziel et al. 2013a, 2013b). The CSS is displaced independently from South
224 Georgia in Dalziel et al., (2013b). The Scotia plate and the ASSA are not present in the reconstructions of
225 Eagles and Jokat (2014) and Livermore et al. (2007), although both Eagles and Jokat and Dalziel et al.
226 (2013a, 2013b) report the presence of the CSS at this stage.

227

228 **4.3 35 Ma- onset of the formation of the ASSA**

229 The ongoing back-arc extension in the region caused sea-floor spreading between the crustal fragments that
230 compose the SSR and the formation of Protector Basin (Fig. 3e and 3f). This has been reported in both
231 Eagles and Jokat (2014)(Fig. 3f) and Livermore et al. (2007) (Fig. 3e). Livermore et al. (2007) treat the
232 South American plate and Tierra del Fuego as one large GU, whereas Eagles et al., (2014) include an
233 extending basin between Tierra del Fuego and the South American plate reported by Ghiglione et al. (2008),
234 resulting in a widening of the underlap with 100km. However, they cannot distinguish how much of the

235 underlap is the result of the errors expected from the rotations of the South American and Antarctic plates
236 in their reconstructions.

237 Pearce et al. (2014) have published a schematic reconstruction that describes the evolution of the ASSA
238 starting at 34 Ma. Pearce et al. (2014) suggest that subduction initiated at the ASSA around 34 Ma, along
239 the eastern margin of the CSS, that was already present at this stage in their reconstruction. Remnants of
240 the southern extend of the subducting slab below the ASSA have been observed in mantle tomography
241 models (Beniest and Schellart, 2020). Galindo-Zaldívar et al., (2006) report Early Miocene ages for the
242 opening of Protector basin, and a Late Oligocene to Early Miocene age for the opening of Dove basin
243 (Galindo-Zaldívar et al., 2014). According to Pearce et al. (2014), the opening of Dove basin and Protector
244 basin follow the initiation of the subduction zone, which is in line with the ages proposed by Galindo-
245 Zaldívar et al. (2006, 2014). These openings are much younger than reported in Eagles and Jokat (2014)
246 and Livermore et al., (2007).

247

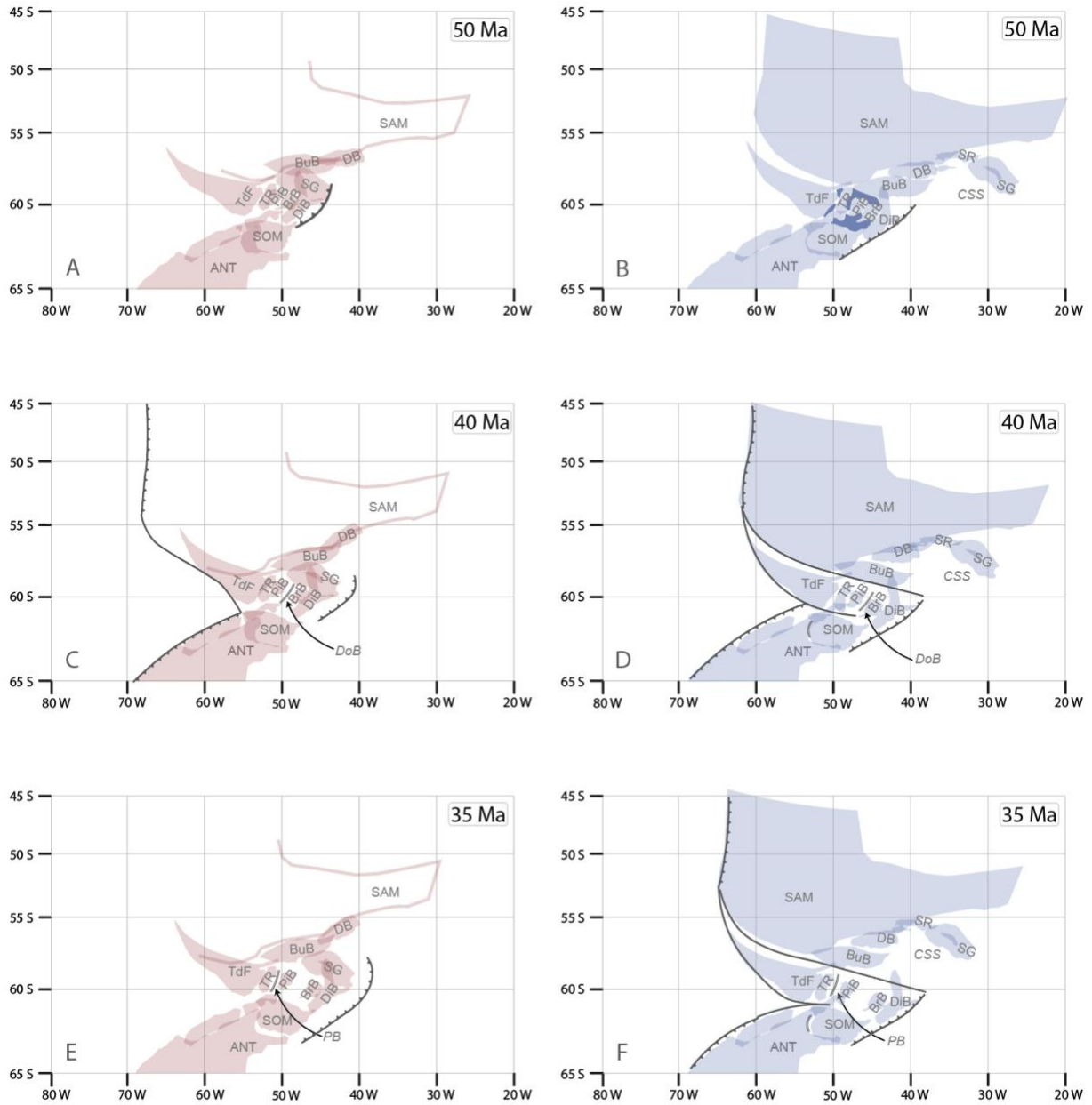
248 **4.4 30 Ma- The ASSA and the possible onset of north-south oriented back arc spreading**

249 The most striking and controversial differences between the compared paleogeographic reconstructions
250 become apparent around 30 Ma (Fig. 3a and 3b). Although all the compared reconstructions agree on the
251 presence of a curved subduction zone at this stage, the influence of the subduction zone on the evolution of
252 the back-arc basin is different. As a consequence of the high curvature of this subduction zone, Livermore
253 et al. (2007) report the initiation of north-south oriented back-arc spreading, eventually leading to the
254 formation of the CSS (Fig. 3a). They also provide evidence for north-south back-arc spreading in the form
255 of east-west striking interpreted isochrons on the seafloor of the CSS, which was suggested by Barker
256 (1970). Eagles and Jokat (2014) (Fig. 3b) have interpreted these anomalies as products of Cretaceous
257 seafloor spreading. They therefore treat the CSS as a rigid crustal block.

258

259

260



261
 262 **Figure 2:** Comparison of the reconstructions (50 Ma – 35 Ma) of Livermore et al. (2007) in red (a, c, e)
 263 and the reconstruction of Eagles and Jokat (2014) in blue (b, d, f), shown with respect to a fixed Antarctica.
 264 Abbreviations in grey are identical to those in figure 1. Subduction and major faults are indicated in black,
 265 sea floor spreading is indicated with two thin black lines when they were presented in the original studies.
 266 The dark blue area in figure 2b represents Omond Land.
 267

274 4.5 25 Ma- Propagation of the WSR

275 From 25 Ma onwards, the northward propagation of the WSR can be observed in the reconstructions of
276 Eagles and Jokat (2014) (Fig. 3d) but is not apparent from the reconstructions of Livermore et al. (2007)
277 (Fig. 3c). Seafloor spreading along the WSR has propagated in the reconstruction of Eagles and Jokat (2014)
278 from the Shackleton Fracture zone towards the eastern side of Burdwood Bank (Fig. 3d). Towards the north,
279 the WSR connects with the remnants of the Burdwood transform fault that runs through Tierra del Fuego.
280 The WSR has not been connected with the NSR yet in the reconstruction of Eagles and Jokat (2014).
281 Livermore et al. (2007) (Fig. 3c) do connect the northernmost transform fault of the WSR to South Georgia.
282 The extent and width of extension in the WSR is smaller in Eagles et al. (2014) compared to Livermore et
283 al. (2007), but the total size of the Scotia plate is larger in the reconstruction of Eagles and Jokat (2014).
284 This results in a subduction zone that is located 150 km further eastward and a more easterly positioned
285 ASSA and South Georgia. Neither the ASSA nor any volcanic activity are mentioned by Livermore et al.
286 (2007). According to Pearce et al. (2014) the ASSA is active over the whole region at 25 Ma, which extends
287 from the south-west corner of South Georgia to the south-east corner of JaB. Although the age, origin and
288 geometry of the CSS are still different between the reconstruction of Pearce et al. (2014) and the
289 reconstructions of Livermore et al. (2007) and Eagles and Jokat (2014), the shape of the subduction zone,
290 the South Sandwich Trench (SST), is similar to that of Eagles and Jokat (2014).

291 Other reconstructions favouring a Cenozoic age for the CSS suggest different ages for the opening of this
292 proposed back-arc basin, and/or do not explain how the propagation of the WSR towards the NSR along
293 the margins of the CSS occurred, as this propagation is unclear in most other reconstructions. The CSS
294 starts opening in a north-south direction shortly after 24 Ma in the reconstruction of V  rard et al. (2012).
295 The CSS does not yet exist in the reconstruction of Nerlich et al. (2013) at 25 Ma but opens shortly after
296 21 Ma. South Georgia remains attached to Discovery Bank and Bruce Bank that do not split up either,
297 which means that Scan Basin is not present in these reconstructions, even though Scan Basin does form in
298 the reconstructions of Livermore et al. (2007) and Eagles and Jokat (2014) at this time step. A CSS that
299 results from Cenozoic back-arc spreading requires a north-south trending transform boundary with the

300 WSS. This boundary is not present in the reconstructions of Barker et al. (2001) nor Livermore et al. (2007)
301 although such a fault is expected. Nerlich et al. (2013) do not mention such a transform boundary but their
302 figure that depicts the age of the Scotia region shows contrasting ages along this assumed transform
303 boundary.

304

305 **4.6 15 Ma- Initiation of spreading along the East Scotia Ridge**

306 There are two major differences between the reconstructions of Eagles and Jokat (2014) and Livermore et
307 al. (2007) at 15 Ma: the extent of the northernmost segment of the WSR, the W7 segment, and the extent
308 of sea-floor spreading during the earliest stage of spreading along ESR (Fig. 3e and 3f). The W7 segment
309 is reconstructed in Eagles and Jokat (2014) (Fig. 3f) but is not reported in Livermore et al. (2007) (Fig. 3e).
310 The ESR comprises of a short ridge (app. 270 km long) striking app. N-S which is located west of the
311 subduction zone in Livermore et al. (2007), while the spreading ridge extends from South Georgia towards
312 Jane Basin in Eagles and Jokat (2014), with a total length of app. 900 km.

313 South Georgia is located 300 km towards the south-west in the reconstruction of Livermore et al. (2007) as
314 a result of the ongoing opening of CSS. Spreading along the ESR starts soon after 20 Ma in the
315 reconstruction of Livermore et al. (2007) (Fig. 3e). Eagles and Jokat (2014) (Fig. 3f) have proposed a similar
316 onset for spreading at the ESR, starting at 17 Ma and the spreading ridge is connected with the spreading
317 ridge in Jane Basin, in contrast to the reconstruction of Pearce et al. (2014), where spreading in Jane Basin
318 already stopped before 20 Ma. Bohoyo et al., (2002) report a cessation of the spreading centre in JaB at
319 14.4 Ma. In the reconstruction of Eagles and Jokat (2014) (Fig. 3f) the spreading centre in Jane Basin is not
320 interrupted when crossing the SSR and continues into Scan Basin. A small transform fault that cuts through
321 Discovery Bank connects this spreading centre in Scan Basin with the ESR. The ESR ends in the
322 reconstruction of Eagles and Jokat (2014) south of South Georgia with a second transform fault, that
323 connects the ESR with the SST. In the model of Pearce et al. (2014) the cessation of spreading in Jane Basin
324 is followed by a period of ongoing subduction of the South American plate. The spreading centre in Jane
325 Basin is cut-off in the north by the SSR strike-slip zone, which merged with a major transform fault in the

326 Weddell Sea oceanic crust. North of this strike-slip fault, spreading continues west of Discovery Bank, in
327 Scan Basin. The spreading continues towards the north. No reference frame has been provided in the
328 reconstruction of Pearce et al. (2014), so the position of the ESR, relative to the other reconstructions, is
329 unclear.

330 No signs of extension along the ESR are visible in the reconstructions of V  rard et al. (2012) at this time
331 step. Nerlich et al. (2013) and Livermore et al. (2007) both did not publish a time slice that can be compared
332 with the 15 Ma time slice. Our reconstruction allows a simulation of the paleo-location of the GUs for the
333 reconstruction of the Livermore et al. (2007) (Fig. 3e), which suggests the ESR has developed significantly
334 at 10 Ma, implying that the ESR has started to spread at 15 Ma, which coincides with the model of Barker
335 (2001).

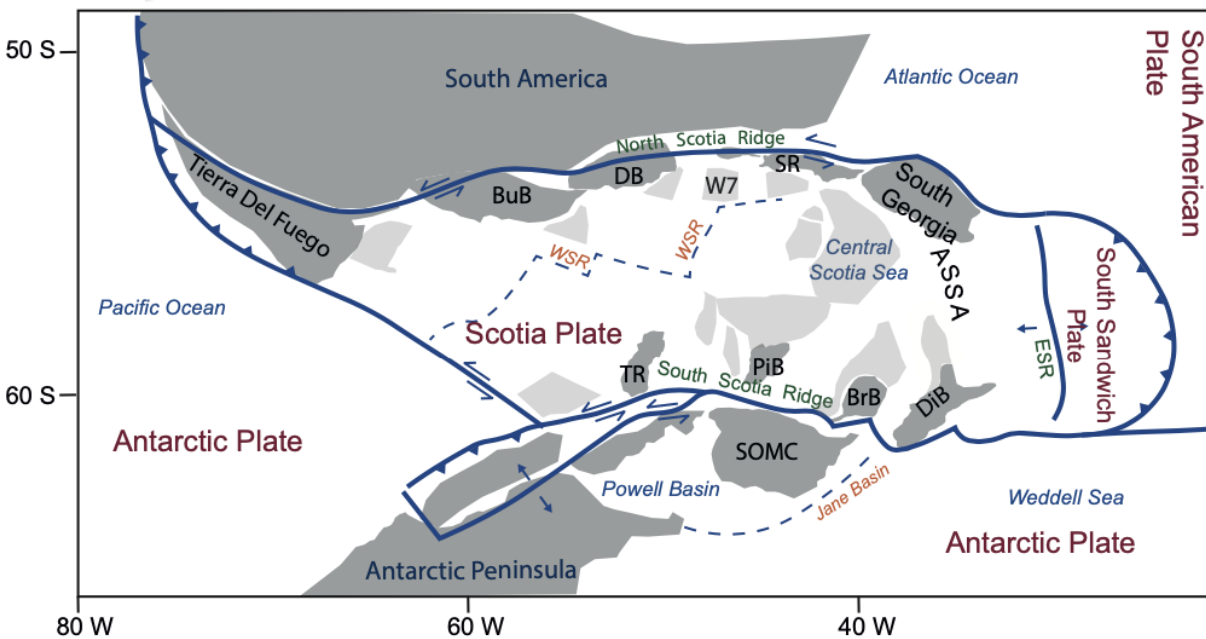
336 The WSR is still spreading at 15 Ma according to Livermore et al. (2007), but they do not show the final
337 stage of WSR evolution. It is therefore unclear if the WSR has ever connected with the NSR in their
338 reconstruction. The same applies to the reconstruction of V  rard et al. (2012). Eagles and Jokat (2014) do
339 connect the WSR to the NSR, which exerts tension on the NSR west of Shag Rocks and thus the formation
340 of the W7 segment.

341

342 **4.7 10 Ma- Present day. End of spreading along the West Scotia Ridge and ongoing spreading along** 343 **the East Scotia Ridge.**

344 At this time slice, close to today's configuration, the compared reconstructions disagree significantly (Fig.
345 3g and 3h). The GUs in the youngest time slice of Livermore et al. (2007) (Fig. 3g) are very different from
346 the reconstruction of Eagles and Jokat (2014) (Fig. 3h). This is most apparent from the position of the GU
347 of South Georgia. To make the connection from 10 Ma to today's configuration the GUs of Livermore et
348 al. (2007) had to be radially dispersed from their 10 Ma positions by rotating and expanding the GUs to
349 their present-day location. In other words, South Georgia had to move around 250 kilometres towards the
350 north-east, the GUs along the SSR towards the south and the SST had to move towards the east. Livermore
351 et al. (2007) (Fig. 3g) propose that the SST has diverted from its previous location along the ASSA, resulting

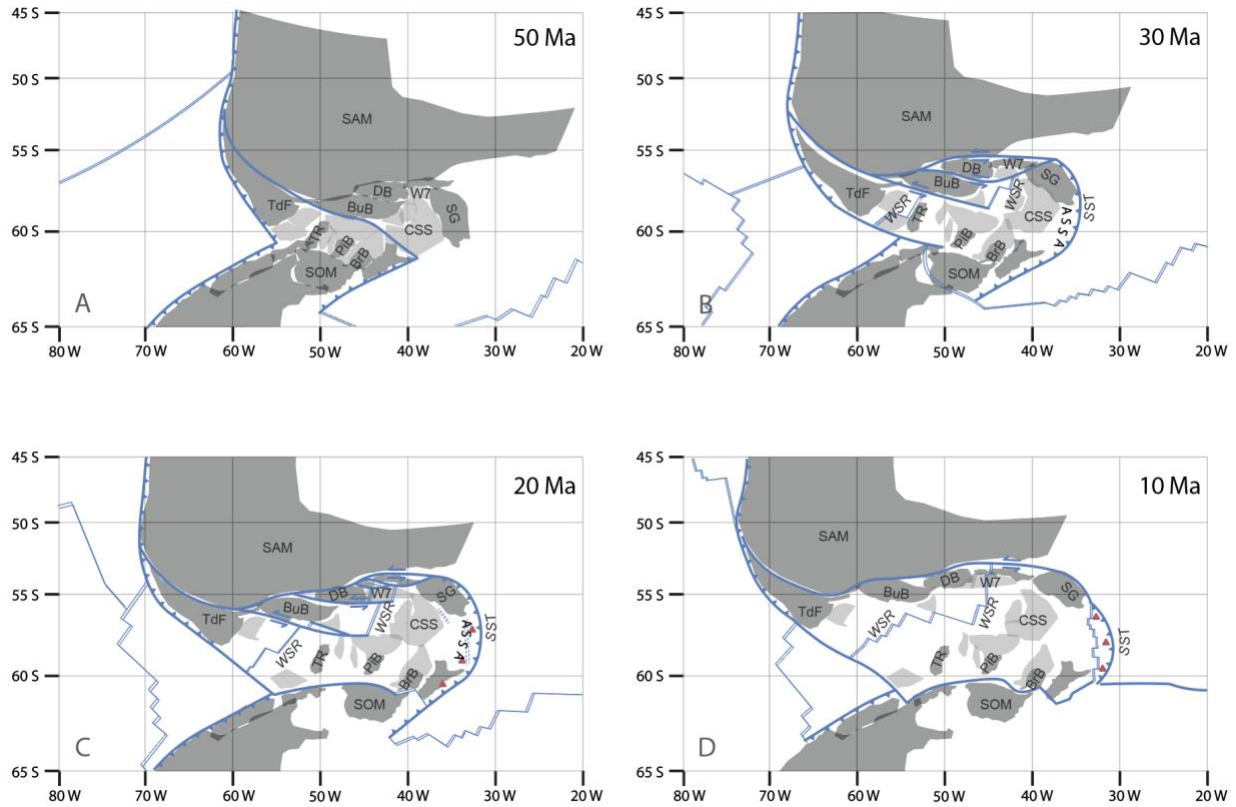
352 in a new arc. The SST has now become a N-S trending curved subduction zone, like its present-day shape.
 353 This is different in the reconstruction of Eagles and Jokat (2014) (Fig. 3h), where the ESR is actively
 354 spreading at 10 Ma, while the SST is still attached to the NSR strike-slip zone. At the 6 Ma timestep of the
 355 reconstruction of Eagles and Jokat (2014) this changes, when a new arc separated from the ASSA is clearly
 356 visible. Pearce et al. (2014) have modelled this separation of the two arcs between 12 Ma and 8 Ma. Dalziel
 357 et al. (2013a, 2013b) suggested the onset of spreading along the ESR at 10 Ma indicated with a few dashed
 358 lines. It is unclear if these dashed lines mark the start of the ESR or if they are a hint to the extension that
 359 might have pre-dated the sea-floor spreading (Dalziel et al., 2013a, 2013b). The development of the
 360 Shackleton Fracture Zone is thought to have caused an eastward asthenospheric mantle flow below the
 361 Scotia Sea region, which halted spreading at the WSR around 6 Ma (Martos et al., 2014b).
 362



363
 364 **Figure 4:** Geological units (GUs) according to their present-day position. The dark grey GUs are
 365 continental fragments and are the same as those used in figure 2 and figure 3. The light grey GUs are newly
 366 defined and interpreted to originate from PPWS. Abbreviations are identical to figure 1. The present-day
 367 tectonic structures are derived from Riley et al. (2019).

368 **5. New Reconstruction**

369 The comparison of reconstructions shows that there is still no agreement on the age and origin of the CSS.
370 The two prevailing end-member solutions consider either a Cretaceous or Cenozoic age of the CSS. The
371 origin of the CSS is considered either as the conjugate of the Weddell Sea or as a back-arc basin. To reach
372 a consensus we present a new tectonic reconstruction including newly identified crustal fragments (see
373 methods). In this reconstruction we bridge the two end-member models including both ages and origins of
374 the CSS as proposed by Livermore et al. (2007) and Eagles and Jokat (2014) (Fig. 5). In our reconstruction,
375 we assume that the CSS and the newly recognised oceanic crustal fragments (Fig. 4) originated in a branch
376 of a gateway that connected the Paleo-Pacific Ocean with the Rocas Verdes Basin and the Weddell Sea
377 (Fig. 6). We hereafter call this gateway the Paleo-Pacific Weddell Sea (PPWS) gateway. A continuous
378 extensional system from the Rocas Verdes Basin to the Weddell Sea has already been proposed by several
379 authors (Eagles, 2010a, 2016; Eagles & Eisermann, 2020; König & Jokat, 2006; Malkowski et al., 2016).
380 Riley et al. (2019) identified Cretaceous crust along the west Scotia Ridge, the W7 segment. We follow
381 their interpretations that this segment was part of the Cretaceous CSS as defined by Eagles and Jokat (2014).
382 Despite the recognition of a continuous branch between the Rocas Verdes Basin and the Weddell Sea, there
383 are no published reconstructions yet that advocate for a CSS containing both Cretaceous crust and Cenozoic
384 crust. In our reconstruction, we include both the GUs that we used to compare the reconstructions of Eagles
385 and Jokat (2014) and Livermore et al. (2007) and the GUs that were once located in an east-west oriented
386 branch between the Weddell Sea and the Paleo-Pacific Ocean at 50 Ma (PPWS gateway Fig. 5a and Fig.
387 6).



388

389 **Figure 5:** New tectonic reconstructions. a) 50 Ma: The Scotia Sea region illustrating the connection
 390 between South America and Antarctica including the paleo-position of the remnants of the PPWS. b) 30
 391 Ma: Scotia Sea region at the start of the formation of the Central Scotia Sea back-arc basin. c) 20 Ma: wide-
 392 spread extension in the Scotia Sea region in response to the retreat of the SST. d) 10 Ma: wide-spread
 393 extension in the Scotia Sea region has ceased, and extension is now centred along the ESR. *Transparent*
 394 *light grey areas represent geological units originating from the PPWS. Subduction, sea floor spreading*
 395 *and major faults are indicated in blue. Volcanism is schematically illustrated with red triangles.*
 396 *Abbreviations are identical to figure 1. Plate boundaries are adapted from Matthews et al.(2016) . The*
 397 *dark grey colours indicate the same crustal blocks as presented in figures 2 and 3.*

398 **5.1. 50 Ma:**

399 In our model, at 50 Ma, a narrow gateway that connects the Paleo-Pacific Ocean and the Weddell Sea
 400 separates South America from Antarctica (Fig. 5a). The GUs originating from this branch are positioned in

401 a seaway between the South American and Antarctic plates, which is different from all previous
402 reconstructions. One could argue that the CSS in the reconstruction of Eagles and Jokat (2014) originates
403 from this branch as well, but the CSS and South Georgia are positioned 350-400 km towards the east in
404 their reconstruction, outside the land bridge. In our reconstruction South Georgia is located much closer to
405 Burdwood Bank and Tierra del Fuego, which is more in agreement with the position proposed by Dalziel
406 et al. (2021). The GUs that will later form the CCS comprise a smaller area in comparison to Eagles and
407 Jokat (2014). We agree with Eagles and Jokat (2014) that there are still two subduction zones active, one
408 on the eastern side and another on the western side of the South American - Antarctic connection during
409 the early Cenozoic (Fig. 5a).

410

411 **5.2: 30 Ma:**

412 We adopt the commonly accepted curved geometry of the SST at 30 Ma (Fig. 5b). This subduction zone was
413 fully developed, with the ASSA representing the active volcanic arc at 30 Ma (Pearce et al., 2014). Apart from
414 the arc, this subducting plate at the ASSA caused stretching in the overriding plate, preluding the initiation of
415 back arc spreading at the WSR. Crustal extension starts in the northern part of the future Scotia Plate, along
416 with what will become the WSR, and close to the arc in the south that will become Jane Basin. The
417 displacement in the north occurs along strike-slip faults.

418

419 **5.3: 20 Ma:**

420 At 20 Ma, back-arc spreading at the West Scotia Ridge is still ongoing with sea floor spreading along the WSR
421 and propagation of the West Scotia Ridge towards the south, following Eagles and Jokat (2014). Several
422 transform faults inside the West Scotia Sea accommodate east-west directed seafloor spreading. We follow
423 Eagles and Jokat (2014) by initiating spreading at the ESR around 20 Ma (Fig. 5c)
424 In our reconstruction (Fig. 5c) the area in between the northern WSR and the ESR experiences extension,
425 which results in stretching in the CSS domain and in South Georgia separating in an anti-clockwise rotation,

426 away from the CSS. This results in a app. 100 km wide bathymetric low between South Georgia and the CSS
427 as well as other areas where the Cretaceous pieces of crust actively thin, and potentially break apart, forming
428 new oceanic crust at poorly developed spreading centres, of Cenozoic age in the CSS. Absence of dredge
429 material to test if there is indeed thinned continental material at the base of these bathymetric lows, make it
430 difficult to confirm this hypothesis. Beniest and Schellart, (2020) map small bits of continental crust in that
431 domain that points to more felsic material than mafic, which they infer from the geophysical signature in the
432 region. Refraction seismic data in this area would help to constrain the crustal structure towards the south-west
433 of South Georgia, but such data are currently absent.

434 The ASSA is still active at 20 Ma and follows the curvature of the subducting slab (Pearce et al., 2014). The
435 retreating slab continues to deform the Scotia Plate. Displacement along strike-slip faults in the NSR and basin
436 opening along the SSR (Protector Basin, Dove Basin and Scan Basin) continues.

437

438 **5.4 10 Ma: spreading along the East Scotia Ridge, formation of the Sandwich plate and eastward retreat** 439 **of the SST**

440 At 10 Ma, extension in the CSS domain starts to cease and continues to be accommodated along the ESR,
441 causing growth of the Sandwich Plate (Fig. 5d). The strike-slip motion along the NSR and ESR continues.
442 Activity at the ASSA stops around 10 Ma (Pearce et al., 2014) in response to the eastward retreat of the
443 subduction zone that led to the formation of the East Scotia Sea back-arc basin and the South Sandwich
444 volcanic arc.

445

446 **6. Discussion**

447 Our presented reconstruction is novel in three different ways: I) we ascribe a larger role to the connection
448 between the Paleo-Pacific Ocean and the Weddell Sea (PPWS gateway, Fig. 6). II) with our reconstruction we
449 recognize more pieces of Cretaceous seafloor that could be related to the PPWS gateway (Fig. 4). III) our
450 reconstruction (Fig. 5) shows that previously published works, with opposing end-member hypotheses, are
451 compatible when considering points I and II.

452

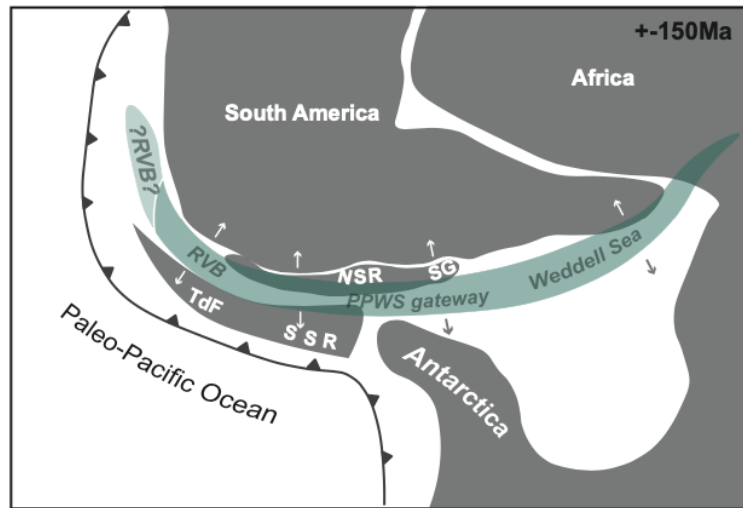
453

454 **6.1 Paleo-Pacific - Weddell Sea (PPWS) gateway**

455 The Weddell Sea and Rocas Verdes Basin both formed during the break-up of southern Gondwana (Eagles,
456 2010a; Jokat et al., 2003; König & Jokat, 2006; Ramos et al., 2020). The Rocas Verdes Basin was located
457 either along the margin of the Paleo-Pacific Ocean (Bastias et al., 2021; Ghiglione, 2016; Schellart et al.,
458 2023; Vérard et al., 2012) or cross-cutting Patagonia at the westernmost extent of the Magallanes - Fagnano
459 Fault System (MFFS, Dalziel et al., 2013a; Dummann et al., 2020; Eagles, 2010a; Maffione et al., 2010;
460 van de Lagemaat et al., 2021). During this initial break-up phase (app. 150 Ma, Bastias et al., 2021; Eagles,
461 2010a; van de Lagemaat et al., 2021), the Weddell Sea spreading centre was possibly connected through an
462 oceanic gateway to the Paleo-Pacific Ocean (Fig. 6), as proposed by multiple authors (Bastias et al., 2021;
463 Dummann et al., 2020; Eagles, 2010b; Ghiglione, 2016; Lagemaat et al., 2021; Vérard et al., 2012). The
464 location and timing of this PPWS gateway is dynamic and starts initially in the Rocas Verdes Basin itself
465 (Dalziel et al., 2013a; Dummann et al., 2020; Eagles, 2010a; van de Lagemaat et al., 2021) after which this
466 branch is abandoned and continues in a proto-Drake Passage just south of mainland Patagonia, Argentina
467 (Dalziel et al., 2013a; Dummann et al., 2020; Eagles, 2010a; Ghiglione, 2016; van de Lagemaat et al.,
468 2021). Other authors (Eagles, 2010a; König & Jokat, 2006) propose that the PPWS gateways are rift- or
469 spreading basins, which implies that the crustal structure would be thinned continental or oceanic crust.

470 In general, it is accepted that continental fragments from the Mesozoic continental parts of South America
471 and Antarctica can be found along the margins of the Scotia Plate. Eagles (2010a), Dalziel et al. (2013a)
472 and Eagles and Jokat (2014) report that parts of the CSS belonged to a more westerly, with respect to the
473 PPWS gateway, located part of the Antarctic conjugate margin, and Riley et al. (2019) hypothesized ‘the
474 existence of a previously unknown volcanic arc on an extension of the adjacent Cretaceous oceanic crust
475 of the CSS’. Magnetic studies identified potential, roughly E-W oriented batholiths in the Central Scotia
476 Sea (Martos et al., 2014). Other than those mentions, no remnants of oceanic or thinned continental crust
477 originating from the PPWS have been reported in the Scotia domain. The recognition of PPWS remnants

478 allowed us to reconstruct the tectonic history of the Scotia Sea domain more elegantly as we will discuss in
 479 the next section.



480
 481 **Figure 6:** Schematic cartoon of the break-up of the southern margin of Gondwana at 150 Ma. Extension is
 482 centred in a zone that extends from the RVB through the PPWS gateway into the Weddell Sea and is
 483 indicated in green. Sea-floor spreading also occurred in the Weddell Sea but is not interpreted in this figure.
 484 Arrows indicate the direction of extension. Modified from (Eagles, 2010b).

485

486 6.2 Provenance of the Scotia Plate seafloor

487 Comparing the same-shaped geological units using the reconstruction of Livermore et al. (2007) and Eagles
 488 and Jokat (2014) revealed that Livermore et al. (2007) (Fig. 2 and 3), who chose an Oligocene age for the
 489 CSS, have a lot of overlap between the GUs (Fig. 2a), whereas Eagles and Jokat (2014), who consider a
 490 Jurassic-Cretaceous age for the CSS, have too much space at 50 Ma in the central part of the land bridge
 491 (Fig. 2b). Livermore et al. (2007) give no explanation for their overlap, but we assume the intention was to
 492 simulate crustal thinning under extension. Eagles and Jokat (2014) recognise Omond-land (Fig. 2b), a
 493 former coastal plain that is now dismembered and scattered over the Scotia Plate, to fill in the gap in their
 494 reconstruction.

495 To overcome the overlap in Livermore et al. (2007) and the underlap in Eagles and Jokat (2014), we have
 496 interpreted the dark grey areas of the Scotia plate (Fig. 4) as remnants of crust originating from the PPWS

497 that got separated during the formation of the Scotia Plate (Fig. 6). Today, these dismembered crustal
498 fragments can be found scattered over the Scotia Plate (Fig. 4), a result of the ongoing back-arc extension
499 since the early Oligocene. This solution gives room for both ideas, where the CSS may consist of older
500 (Cretaceous) crustal material (Dalziel et al., 2013a; Dalziel et al., 2013b; De Wit, 1977; Eagles, 2010a;
501 Eagles and Jokat, 2014), younger crustal material (Barker, 2001; Livermore et al., 2007; Nerlich et al.,
502 2013; V  rard et al., 2012) that formed during an Oligocene-Miocene extension phase and batholith that
503 reside in the crust of the CSS (Martos et al., 2014) around which extension was accommodated. In addition,
504 our solution also explains the Cretaceous ages of dredged rock samples reported by Riley et al. (2019)
505 without generating large amounts of overlap or gaps between GUs as experienced by Livermore et al.
506 (2007) and Eagles and Jokat (2014).

507 We acknowledge that our GUs, which represent continental crust and remain rigid during our reconstructed
508 50 myr, likely underwent some (diffuse) deformation during this time span. The amount of data from this
509 region, which is currently sparse due to a limited number of drilled and dredged samples (see review Beni  st
510 and Schellart, 2020), with the most recent expedition IODP 382 carried out in 2019 (P  rez et al., 2021),
511 should increase to confirm the presence and lateral extent of remnant fragments of the PPWS gateway. The
512 only reconstruction that is suitable for a detailed comparison, that is also reconstructed with a GU that
513 resembles a captured piece of (Cretaceous/oceanic crust) is that of Eagles and Jokat (2014). Other than that,
514 no GUs with an origin related to something like the PPWS gateway have previously been recognized.
515 Therefore, different sizes and shapes are possible, depending on the configuration of these newly identified
516 GUs at 50 Ma.

517

518 **6.3 Implications for the onset of the Antarctic Circumpolar Current**

519 In our reconstruction, we assume that the crustal nature of the newly identified GUs are of oceanic origin
520 and were most likely submerged at 50 Ma. This opens up the possibility for a, potentially shallow, Eocene-
521 age paleo-gateway between the between the Pacific Ocean and the Atlantic Ocean around 50 Ma, which

522 would pre-date the deeper ocean currents that are known to be present after the opening of Drake Passage
523 (Maldonado et al., 2003; Martos et al., 2013).

524 To mitigate this challenge of identifying potential remnants of the PPWS gateway and possible earlier
525 gateways between the Pacific and the Atlantic oceans, more data are required. These data may consist of
526 dredged samples that specifically target the CSS, but it also includes high resolution reflection seismic data
527 on the CSS. Until today, most of the reflection seismic data has been acquired and interpreted in the basins
528 along the SSR (Civile et al., 2012; García et al., 2016; Kavoun & Vinnikovskaya, 1994; Lindeque et al.,
529 2013; Maldonado et al., 1998; Maldonado et al., 2015; Vanneste et al., 2002), which has revealed important
530 constraints on the tectonic movement of crustal blocks along the SSR. The CSS, and specifically the region
531 around South Georgia, remains to be investigated. Apart from reflection seismic data, refraction seismic
532 data would be particularly useful across the CSS, because this type of data allows the analysis of the crustal
533 structure based on seismic velocities, which are quite specific for both felsic and mafic rocks.

534

535 **7. Conclusion**

536 The paleogeographic comparisons and remodelling of published reconstructions of the tectonic evolution
537 of the Scotia region highlight important similarities and striking differences. A reinterpretation of these
538 reconstructions in combination with bathymetric and magnetic anomaly data implies that pieces of
539 Cretaceous crust are scattered throughout the CSS and along the margins of the NSR and SSR as a result
540 of Cenozoic back-arc extension.

541 To compare existing models, we redefined GUs and remodelled existing reconstructions describing the
542 Cenozoic evolution of the Scotia region. This comparison shows that major differences between the
543 reconstructions exist in the age, origin and extent of the CSS and the role of the subducting SAM plate.

544 We propose a hybrid tectonic model, challenging the idea of a purely Cretaceous or Cenozoic age crust of
545 the CSS. We also identify more regions that are potentially made of Cretaceous oceanic crust or stretched
546 continental crust along the margins of the CSS and along the NSR and SSR. The areas containing such crust

547 originate from crustal extension and seafloor spreading in the PPWS, which formed during the first phase
548 of rifting and break-up of southern Gondwanaland. Most of the expansion of the CSS back-arc basin
549 occurred during the Oligocene and Miocene in response to westward subduction of the South American
550 plate under the Scotia plate. To verify this reconstruction, more geological and geophysical data about the
551 age and lithology of the remnants of the PPWS gateway should be acquired, for example by dredging the
552 sea floor of those areas or acquiring reflection and/or refraction seismic data.

553

554 **8. Acknowledgements:**

555 This work was supported by a Vici Fellowship (016.VICI.170.110) awarded to W.P. Schellart. The authors
556 would like to thank Graeme Eagles for the constructive reviews on an earlier version of the manuscript.

557

558 **9. Open Research**

559 No new data were generated or used during this project.

560 **10. References**

561 Anagnostou, E., John, E. H., Edgar, K. M., Foster, G. L., Ridgwell, A., Inglis, G. N., et al. (2016).

562 Changing atmospheric CO₂ concentration was the primary driver of early Cenozoic climate. *Nature*,
563 533(7603), 380–384. <https://doi.org/10.1038/nature17423>

564 Barker, P. F. (1972). A spreading centre in the east Scotia sea. *Earth and Planetary Science Letters*,
565 15(2), 123–132. [https://doi.org/10.1016/0012-821X\(72\)90052-0](https://doi.org/10.1016/0012-821X(72)90052-0)

566 Barker, P F. (1970). Plate Tectonics of the Scotia Sea region. *Nature*, 228, 1293–1296.

567 Barker, P F, & Burrell, J. (1977). The problem of Drake Passage opening has significance outside the

568 field of regional tectonics : the creation of a continuous circum-Antarctic deep- water path in the

569 zone of the mid-latitude westerly winds -- by separation from Antarctica of South America. *Marine*

570 *Geology*, 25, 15–34.

- 571 Barker, Peter F. (2001). *Scotia sea regional tectonic evolution: implications for mantle flow and*
572 *palaeocirculation. Earth Science Reviews* (Vol. 55). [https://doi.org/10.1016/S0012-8252\(01\)00055-](https://doi.org/10.1016/S0012-8252(01)00055-1)
573 [1](https://doi.org/10.1016/S0012-8252(01)00055-1)
- 574 Barker, Peter F., Filippelli, G. M., Florindo, F., Martin, E. E., & Scher, H. D. (2007). Onset and role of
575 the Antarctic Circumpolar Current. *Deep-Sea Research Part II: Topical Studies in Oceanography*,
576 *54*(21–22), 2388–2398. <https://doi.org/10.1016/j.dsr2.2007.07.028>
- 577 Bastias, J., Spikings, R., Riley, T., Ulianov, A., Grunow, A., Chiaradia, M., & Hervé, F. (2021). A revised
578 interpretation of the Chon Aike magmatic province: Active margin origin and implications for the
579 opening of the Weddell Sea. *Lithos*, *386–387*. <https://doi.org/10.1016/j.lithos.2021.106013>
- 580 Beniest, A., & Schellart, W. P. (2020). A geological map of the Scotia Sea area constrained by
581 bathymetry, geological data, geophysical data and seismic tomography models from the deep
582 mantle. *Earth-Science Reviews*, *210*(October), 103391.
583 <https://doi.org/10.1016/j.earscirev.2020.103391>
- 584 Bijl, P. K., Bendle, J. A. P., Bohaty, S. M., Pross, J., Schouten, S., & Tauxe, L. (2013). Eocene cooling
585 linked to early flow across the Tasmanian Gateway, *110*(24).
586 <https://doi.org/10.1073/pnas.1220872110>
- 587 Bohoyo, F., Maldonado, A., Schreider, A. A., Suriñach, E., & Galindo-Zaldívar, J. (2002). Basin
588 development subsequent to ridge-trench collision: the Jane Basin, Antarctica. *Marine Geophysical*
589 *Research*, 413–421.
- 590 Bohoyo, F., Larter, R. D., Galindo-Zaldívar, J., Leat, P. T., Maldonado, A., Tate, A. J., et al. (2019).
591 Morphological and geological features of Drake Passage, Antarctica, from a new digital bathymetric
592 model. *Journal of Maps*, *15*(2), 49–59. <https://doi.org/10.1080/17445647.2018.1543618>
- 593 Boyden, J. A., Müller, R. D., Gurnis, M., Torsvik, T. H., Clark, J. A., Turner, M., et al. (2011). Next-
594 generation plate-tectonic reconstructions using GPlates. In *Geoinformatics: Cyberinfrastructure for*
595 *the Solid Earth Sciences* (Vol. 9780521897, pp. 95–114).
596 <https://doi.org/10.1017/CBO9780511976308.008>

- 597 Civile, D., Lodolo, E., Vuan, A., & Loreto, M. F. (2012). Tectonics of the Scotia-Antarctica plate
598 boundary constrained from seismic and seismological data. *Tectonophysics*, 550–553, 17–34.
599 <https://doi.org/10.1016/j.tecto.2012.05.002>
- 600 Cunningham, A. P., Barker, P. F., & Tomlinson, J. S. (1998). Tectonics and sedimentary environment of
601 the North Scotia Ridge region revealed by side-scan sonar. *Journal of the Geological Society*,
602 155(6), 941–956. <https://doi.org/10.1144/gsjgs.155.6.0941>
- 603 Dalziel, I. W.D. (1983). The evolution of the Scotia arc: a review (Antarctica). *Antarctic Earth Science*.
604 *4th International Symposium*, 283–288.
- 605 Dalziel, I. W.D., Lawver, L. A., Pearce, J. A., Barker, P. F., Hastie, A. R., Barfod, D. N., et al. (2013a). A
606 potential barrier to deep antarctic circumpolar flow until the late miocene? *Geology*, 41(9), 947–950.
607 <https://doi.org/10.1130/G34352.1>
- 608 Dalziel, Ian W.D., Lawver, L. A., Norton, I. O., & Gahagan, L. M. (2013b). The Scotia arc: Genesis,
609 evolution, global significance. *Annual Review of Earth and Planetary Sciences*, 41, 767–793.
610 <https://doi.org/10.1146/annurev-earth-050212-124155>
- 611 Dalziel, Ian W.D., Macdonald, D. I. M., Stone, P., & Storey, B. C. (2021). South Georgia microcontinent:
612 Displaced fragment of the southernmost Andes. *Earth-Science Reviews*, 220(March), 103671.
613 <https://doi.org/10.1016/j.earscirev.2021.103671>
- 614 Dummann, W., Steinig, S., Hofmann, P., Flögel, S., Osborne, A. H., Frank, M., et al. (2020). The impact
615 of Early Cretaceous gateway evolution on ocean circulation and organic carbon burial in the
616 emerging South Atlantic and Southern Ocean basins. *Earth and Planetary Science Letters*, 530,
617 115890. <https://doi.org/10.1016/j.epsl.2019.115890>
- 618 Eagles, G. (2000). Modelling Plate Kinematics in the Scotia Sea, (September), 1–327.
- 619 Eagles, G. (2010a). South Georgia and Gondwana’s Pacific Margin: Lost in translation? *Journal of South*
620 *American Earth Sciences*, 30(2), 65–70. <https://doi.org/10.1016/j.jsames.2010.04.004>
- 621 Eagles, G. (2010b). The age and origin of the central Scotia Sea. *Geophysical Journal International*,
622 183(2), 587–600. <https://doi.org/10.1111/j.1365-246X.2010.04781.x>

- 623 Eagles, G. (2016). Plate kinematics of the Rocas Verdes Basin and Patagonian orocline. *Gondwana*
624 *Research*, 37, 98–109. <https://doi.org/10.1016/j.gr.2016.05.015>
- 625 Eagles, G., & Eisermann, H. (2020). The Skytrain plate and tectonic evolution of southwest Gondwana
626 since Jurassic times. *Scientific Reports*, 1–17. <https://doi.org/10.1038/s41598-020-77070-6>
- 627 Eagles, G., & Jokat, W. (2014). Tectonic reconstructions for paleobathymetry in Drake Passage.
628 *Tectonophysics*, 611, 28–50. <https://doi.org/10.1016/j.tecto.2013.11.021>
- 629 Eagles, G., Livermore, R. A., Fairhead, J. D., & Morris, P. (2005). Tectonic evolution of the west Scotia
630 Sea. *Journal of Geophysical Research: Solid Earth*, 110(2), 1–19.
631 <https://doi.org/10.1029/2004JB003154>
- 632 Eagles, G., Livermore, R., & Morris, P. (2006). Small basins in the Scotia Sea: The Eocene Drake
633 Passage gateway. *Earth and Planetary Science Letters*, 242(3–4), 343–353.
634 <https://doi.org/10.1016/j.epsl.2005.11.060>
- 635 Galindo-Zaldívar, J., Bohoyo, F., Maldonado, A., Schreider, A., Suriñach, E., & Vázquez, J. T. (2006).
636 Propagating rift during the opening of a small oceanic basin: The Protector Basin (Scotia Arc,
637 Antarctica). *Earth and Planetary Science Letters*, 241(3–4), 398–412.
638 <https://doi.org/10.1016/j.epsl.2005.11.056>
- 639 Galindo-Zaldívar, J., Puga, E., Bohoyo, F., González, F. J., Maldonado, A., Martos, Y. M., et al. (2014).
640 Reprint of “Magmatism, structure and age of Dove Basin (Antarctica): A key to understanding
641 South Scotia Arc development.” *Global and Planetary Change*, 123, 249–268.
642 <https://doi.org/10.1016/j.gloplacha.2014.11.002>
- 643 García, M., Lobo, F. J., Maldonado, A., Hernández-Molina, F. J., Bohoyo, F., & Pérez, L. F. (2016).
644 High-resolution seismic stratigraphy and morphology of the Scan Basin contourite fan, southern
645 Scotia Sea, Antarctica. *Marine Geology*, 378, 361–373.
646 <https://doi.org/10.1016/j.margeo.2016.01.011>
- 647 Ghiglione, M. C. (2016). *Orogenic Growth of the Fuegian Andes (52–56°) and Their Relation to*
648 *Tectonics of the Scotia Arc*. https://doi.org/10.1007/978-3-319-23060-3_11

- 649 Ghiglione, M. C., Yagupsky, D., Ghidella, M., & Ramos, V. A. (2008). Continental stretching preceding
650 the opening of the Drake Passage: Evidence from Tierra del Fuego. *Geology*, *36*(8), 643–646.
651 <https://doi.org/10.1130/G24857A.1>
- 652 Heezen, B. C., & Johnson, G. L. (1965). The South Sandwich Trench. *Deep-Sea Research*, *12*(776), 185–
653 197. [https://doi.org/10.1016/0011-7471\(65\)90024-0](https://doi.org/10.1016/0011-7471(65)90024-0)
- 654 Hill, I. A., & Barker, P. F. (1980). Evidence for Miocene back-arc spreading in the central Scotia Sea.
655 *Geophysical Journal of the Royal Astronomical Society*, *63*(2), 427–440.
656 <https://doi.org/10.1111/j.1365-246X.1980.tb02630.x>
- 657 Hogg, O. T., Huvenne, V. A. I., Griffiths, H. J., Dorschel, B., & Linse, K. (2016). Landscape mapping at
658 sub-Antarctic South Georgia provides a protocol for underpinning large-scale marine protected
659 areas. *Scientific Reports*, *6*(August), 1–15. <https://doi.org/10.1038/srep33163>
- 660 Jokat, W., Boebel, T., König, M., & Meyer, U. (2003). Timing and geometry of early Gondwana breakup.
661 *Journal of Geophysical Research*, *108*(B9), 2428. <https://doi.org/10.1029/2002JB001802>
- 662 Kavoun, M., & Vinnikovskaya, O. (1994). Seismic stratigraphy and tectonics of the northwestern
663 Weddell Sea (Antarctica) inferred from marine geophysical surveys. *Tectonophysics*, *240*(1–4),
664 299–341. [https://doi.org/10.1016/0040-1951\(94\)90277-1](https://doi.org/10.1016/0040-1951(94)90277-1)
- 665 Kennett, J. P. (1977). Cenozoic evolution of Antarctic glaciation, the Circum-Antarctic Ocean and their
666 impact on global paleoceanography. *Journal of Geophysical Research*, *82*(27), 3843–3860.
- 667 König, M., & Jokat, W. (2006). The Mesozoic breakup of the Weddell Sea. *Journal of Geophysical*
668 *Research: Solid Earth*, *111*(B12), n/a-n/a. <https://doi.org/10.1029/2005jb004035>
- 669 Lagemaat, S. H. A. Van De, Swart, M. L. A., Vaes, B., Kusters, M. E., Boschman, L. M., Burton-
670 johnson, A., et al. (2021). Earth-Science Reviews Subduction initiation in the Scotia Sea region and
671 opening of the Drake Passage : When and why ? *Earth-Science Reviews*, *215*(October 2020),
672 103551. <https://doi.org/10.1016/j.earscirev.2021.103551>
- 673 Larter, R. D., Vanneste, L. E., Morris, P., & Smythe, D. K. (2003). Structure and tectonic evolution of the
674 South Sandwich arc. *Geological Society Special Publication*, *219*, 255–284.

- 675 <https://doi.org/10.1144/GSL.SP.2003.219.01.13>
- 676 Lawver, L. A., & Gahagan, L. M. (2003). Evolution of Cenozoic seaways in the circum-Antarctic region.
677 *Palaeogeography, Palaeoclimatology, Palaeoecology*, 198(1–2), 11–37.
678 [https://doi.org/10.1016/S0031-0182\(03\)00392-4](https://doi.org/10.1016/S0031-0182(03)00392-4)
- 679 Leat, P. T., Fretwell, P. T., Tate, A. J., Larter, R. D., Martin, T. J., Smellie, J. L., et al. (2016). Bathymetry
680 and geological setting of the South Sandwich Islands volcanic arc. *Antarctic Science*, 28(4), 293–
681 303. <https://doi.org/10.1017/S0954102016000043>
- 682 Lindeque, A., Martos, asmina M., Gohl, K., & Maldonado, A. (2013). Deep-sea pre-glacial to glacial
683 sedimentation in the Weddell Sea and southern Scotia Sea from a cross-basin seismic transect.
684 *Marine Geology*, 336, 61–83. <https://doi.org/10.1016/j.margeo.2012.11.004>
- 685 Livermore, R., Nankivell, A., Eagles, G., & Morris, P. (2005). Paleogene opening of Drake Passage.
686 *Earth and Planetary Science Letters*, 236(1–2), 459–470. <https://doi.org/10.1016/j.epsl.2005.03.027>
- 687 Livermore, R., Hillenbrand, C. D., Meredith, M., & Eagles, G. (2007). Drake Passage and Cenozoic
688 climate: an open and shut case? *Geochemistry, Geophysics, Geosystems*, 8, 1–11.
689 <https://doi.org/10.1029/2005GC001224>
- 690 Livermore, R. A., McAdoo, D., & Marks, K. (1994). Scotia Sea tectonics from high-resolution satellite
691 gravity. *Earth and Planetary Science Letters*, 123, 255–268. [https://doi.org/10.1016/0012-
692 821X\(94\)90272-0](https://doi.org/10.1016/0012-821X(94)90272-0)
- 693 Maffione, M., Speranza, F., Faccenna, C., & Rossello, E. (2010). Paleomagnetic evidence for a pre-early
694 Eocene (~ 50 Ma) bending of the Patagonian orocline (Tierra del Fuego, Argentina):
695 Paleogeographic and tectonic implications. *Earth and Planetary Science Letters*, 289(1–2), 273–
696 286. <https://doi.org/10.1016/j.epsl.2009.11.015>
- 697 Maldonado, A., Zitellini, N., Leitchenkoy, G., Balanyá, J. C., Coren, F., Galindo-Zaldívar, J., et al.
698 (1998). Small ocean basin development along the Scotia-Antarctica plate boundary and in the
699 northern Weddell Sea. *Tectonophysics*, 296(3–4), 371–402. [https://doi.org/10.1016/S0040-
700 1951\(98\)00153-X](https://doi.org/10.1016/S0040-7000(98)00153-X)

- 701 Maldonado, A., Bohoyo, F., Galindo-Zaldívar, J., Hernández-Molina, J., Jabaloy, A., Lobo, F. J., et al.
702 (2006). Ocean basins near the scotia-antarctic plate boundary: Influence of tectonics and
703 paleoceanography on the cenozoic deposits. *Marine Geophysical Research*, 27(2), 83–107.
704 <https://doi.org/10.1007/s11001-006-9003-4>
- 705 Maldonado, Andrés, Barnolas, A., Bohoyo, F., Galindo-Zaldívar, J., Hernández-Molina, J., Lobo, F., et
706 al. (2003). Contourite deposits in the central Scotia Sea: the importance of the Antarctic
707 Circumpolar Current and the Weddell Gyre flows. *Palaeogeography, Palaeoclimatology,*
708 *Palaeoecology*, 198(1–2), 187–221. [https://doi.org/10.1016/S0031-0182\(03\)00401-2](https://doi.org/10.1016/S0031-0182(03)00401-2)
- 709 Maldonado, Andrés, Bohoyo, F., Galindo-Zaldívar, J., Hernández-Molina, F. J., Lobo, F. J., Lodolo, E., et
710 al. (2014). A model of oceanic development by ridge jumping: Opening of the Scotia Sea. *Global*
711 *and Planetary Change*, 123, 152–173. <https://doi.org/10.1016/j.gloplacha.2014.06.010>
- 712 Maldonado, Andrés, Dalziel, I. W. D., & Leat, P. T. (2015). The global relevance of the Scotia Arc: An
713 introduction. *Global and Planetary Change*, 125, A1–A8.
714 <https://doi.org/10.1016/j.gloplacha.2014.06.011>
- 715 Malkowski, M. A., Grove, M., & Graham, S. A. (2016). Unzipping the Patagonian Andes-Long-lived
716 influence of rifting history on foreland basin evolution. *Lithosphere*, 8(1), 23–28.
717 <https://doi.org/10.1130/L489.1>
- 718 Martos, Y. M., Maldonado, A., Lobo, F. J., Hernández-Molina, F. J., & Pérez, L. F. (2013). Tectonics and
719 palaeoceanographic evolution recorded by contourite features in southern Drake Passage
720 (Antarctica). *Marine Geology*, 343, 76–91. <https://doi.org/10.1016/j.margeo.2013.06.015>
- 721 Martos, Y. M., Galindo-zaldívar, J., Catalán, M., & Bohoyo, F. (2014). Asthenospheric Pacific-Atlantic
722 flow barriers and the West Scotia Ridge extinction. *Geophysical Research Letters*, 41, 43–49.
723 <https://doi.org/10.1002/2013GL058885>
- 724 Martos, Y. M., Catalán, M., Galindo-Zaldívar, J., Maldonado, A., & Bohoyo, F. (2014). Insights about the
725 structure and evolution of the Scotia Arc from a new magnetic data compilation. *Global and*
726 *Planetary Change*, 123, 239–248. <https://doi.org/10.1016/j.gloplacha.2014.07.022>

- 727 mattoMatthews, K. J., Maloney, K. T., Zahirovic, S., Williams, S. E., Seton, M., & Müller, R. D. (2016).
 728 Global plate boundary evolution and kinematics since the late Paleozoic. *Global and Planetary*
 729 *Change*, *146*, 226–250. <https://doi.org/10.1016/j.gloplacha.2016.10.002>
- 730 Nerlich, R., Clark, S. R., & Bunge, H. P. (2013). The Scotia Sea gateway: No outlet for Pacific mantle.
 731 *Tectonophysics*, *604*, 41–50. <https://doi.org/10.1016/j.tecto.2012.08.023>
- 732 Pearce, J. A., Hastie, A. R., Leat, P. T., Dalziel, I. W., Lawver, L. A., Barker, P. F., et al. (2014).
 733 Composition and evolution of the Ancestral South Sandwich Arc: implications for the flow of deep
 734 ocean water and mantle through the Drake Passage Gateway. *Global and Planetary Change*, *123*,
 735 298–322. <https://doi.org/10.1016/j.gloplacha.2014.08.017>
- 736 Pearson, P. N., Foster, G. L., & Wade, B. S. (2009). Atmospheric carbon dioxide through the Eocene –
 737 Oligocene climate transition. *Nature*, *461*, 1110–1114. <https://doi.org/10.1038/nature08447>
- 738 Pérez, L., Bohoyo, F., Hernández-Molina, F. J., Casas, D., Galindo-Zaldívar, J., Ruano, P., & Maldonado,
 739 A. (2016). Tectonic activity evolution of the Scotia-Antarctic Plate boundary from mass transport
 740 deposit analysis. *Journal of Geophysical Research Solid Earth*, *121*, 2216–2234.
 741 <https://doi.org/10.1002/2015JB012622>.Received
- 742 Pérez, L. F., Maldonado, A., Hernández-Molina, F. J., Lodolo, E., Bohoyo, F., & Galindo. (2017).
 743 Tectonic and oceanographic control of sedimentary patterns in a small oceanic basin: Dove Basin
 744 (Scotia Sea, Antarctica). *Basin Research*, *29*, 255–276.
- 745 Pérez, Lara F., Lodolo, E., Maldonado, A., Hernández-Molina, F. J., Bohoyo, F., Galindo-Zaldívar, J., et
 746 al. (2014). Tectonic development, sedimentation and paleoceanography of the Scan Basin (southern
 747 Scotia Sea, Antarctica). *Global and Planetary Change*, *123*, 344–358.
 748 <https://doi.org/10.1016/j.gloplacha.2014.06.007>
- 749 Pérez, Lara F, Hernández-molina, F. J., Lodolo, E., Bohoyo, F., Galindo-Zaldívar, J., & Maldonado, A.
 750 (2019). Oceanographic and climatic consequences of the tectonic evolution of the southern scotia
 751 sea basins, Antarctica. *Earth-Science Reviews*, *198*, 1–18.
 752 <https://doi.org/10.1016/j.earscirev.2019.102922>

- 753 Pérez, Lara F, Martos, Y. M., García, M., Weber, M. E., Raymo, E., Williams, T., et al. (2021). Miocene
754 to present oceanographic variability in the Scotia Sea and Antarctic ice sheets dynamics : Insight
755 from revised seismic-stratigraphy following IODP Expedition 382. *Earth and Planetary Science*
756 *Letters*, 553, 116657. <https://doi.org/10.1016/j.epsl.2020.116657>
- 757 QGIS, D. T. (2018). QGIS Geographic Information System. Open Source Geospatial Foundation Project.
758 <Http://Www.Qgis.Org/>.
- 759 Ramos, V. A., Naipauer, M., Leanza, H. A., & Sigismondi, M. E. (2020). The Vaca Muerta Formation of
760 the Neuquén Basin: an exceptional setting along the Andean continental margin. *AAPG Memoir*,
761 *120*(October), 13pp. <https://doi.org/10.1306/13682222M1202855>
- 762 Riley, T. R., Carter, A., Leat, P. T., Burton-Johnson, A., Bastias, J., Spikings, R. A., et al. (2019).
763 Geochronology and geochemistry of the northern Scotia Sea: A revised interpretation of the North
764 and West Scotia ridge junction. *Earth and Planetary Science Letters*, 518(May), 136–147.
765 <https://doi.org/10.1016/j.epsl.2019.04.031>
- 766 Ryan, W. B. F., Carbotte, S. M., Coplan, J. O., O’Hara, S., Melkonian, A., Arko, R., et al. (2009). Global
767 Multi-Resolution Topography (GMRT) synthesis data set. *Geochemistry, Geophysics, Geosystems*,
768 *10*(3), Q03014.
- 769 Sandwell, D. T., Müller, R. D., Smith, W. H. F., Garcia, E., & Francis, R. (2014). New global marine
770 gravity model from CryoSat-2 and Jason-1 reveals buried tectonic structure. *Science*, 346(6205),
771 65–67. <https://doi.org/10.1126/science.1258213>
- 772 Sauermilch, I., Whittaker, J. M., Klocker, A., Munday, D. R., Hochmuth, K., Bijl, P. K., & Lacasce, J. H.
773 (2021). Gateway-driven weakening of ocean gyres leads to Southern Ocean cooling. *Nature*
774 *Communications*, 12(6465), 1–8. <https://doi.org/10.1038/s41467-021-26658-1>
- 775 Schellart, W. P., Strak, V., Beniést, A., Duarte, J. C., & Rosas, F. M. (2023). Subduction invasion polarity
776 switch from the Pacific to the Atlantic Ocean: A new geodynamic model of subduction initiation
777 based on the Scotia Sea region. *Earth-Science Reviews*, 236(December 2022), 104277.
778 <https://doi.org/10.1016/j.earscirev.2022.104277>

- 779 Scher, H. D., Whittaker, J. M., Williams, S. E., Latimer, J. C., Kordesch, W. E. C., & Delaney, M. L.
780 (2015). Onset of Antarctic Circumpolar Current 30 million years ago as Tasmanian Gateway aligned
781 with westerlies. *Nature*, *523*(7562), 580–583. <https://doi.org/10.1038/nature14598>
- 782 Smalley, J., Dalziel, I. W. D., Bevis, M. G., Kendrick, E., Stamps, D. S., King, E. C., et al. (2007). Scotia
783 arc kinematics from GPS geodesy. *Geophysical Research Letters*, *34*(21), 1–6.
784 <https://doi.org/10.1029/2007GL031699>
- 785 Tanner, P. W. P. (1982). Geology of Shag Rocks, part of a continental block on the north Scotia Ridge,
786 and possible regional correlations. *British Antarctic Survey Bulletin*.
- 787 Vanneste, L. E., Larter, R. D., & Smythe, D. K. (2002). Slice of intraoceanic arc: Insights from the first
788 multichannel seismic reflection profile across the South Sandwich island arc. *Geology*, *30*(9), 819–
789 822. [https://doi.org/10.1130/0091-7613\(2002\)030<0819:SOIAIF>2.0.CO;2](https://doi.org/10.1130/0091-7613(2002)030<0819:SOIAIF>2.0.CO;2)
- 790 V erard, C., Flores, K., & Stampfli, G. (2012). Geodynamic reconstructions of the South America-
791 Antarctica plate system. *Journal of Geodynamics*, *53*(1), 43–60.
792 <https://doi.org/10.1016/j.jog.2011.07.007>
- 793 Weatherall, P., Marks, K. M., Jakobsson, M., Schmitt, T., Tani, S., Arndt, J. E., et al. (2015). A new
794 digital bathymetric model of the world’s oceans. *Earth and Space Science*, *2*, 331–345.
795 <https://doi.org/10.1002/2015EA000107>.Received
- 796 Whitworth, T. (1983). Monitoring the Transport of the Antarctic Circumpolar Current at Drake Passage.
797 *Journal of Physical Oceanography*. [https://doi.org/10.1175/1520-](https://doi.org/10.1175/1520-0485(1983)013<2045:mttota>2.0.co;2)
798 [0485\(1983\)013<2045:mttota>2.0.co;2](https://doi.org/10.1175/1520-0485(1983)013<2045:mttota>2.0.co;2)
- 799 De Wit, M. J. (1977). The evolution of the Scotia Arc as a key to the reconstruction of southwestern
800 Gondwanaland. *Tectonophysics*, *37*(1–3), 53–81. [https://doi.org/10.1016/0040-1951\(77\)90039-7](https://doi.org/10.1016/0040-1951(77)90039-7)
801